NASA TECHNICAL TRANSLATION NASA TT F-14,053

ANODE EFFECT AND GRAPHITE FLUORIDE

W. Nobuatsu and A. Teruaki

Translation of: "Yokyoku koka to fukka kokuen",
Denki kagaku, Vol. 39, No. 2, 1971, pp. 123-130.
(Journal of the Electrochemical Society of Japan)

NATIONAL AERONAUTICS AND SPACE ADMINISTRATION
WASHINGTON, D.C. 20546 DECEMBER 1971

ANODE EFFECT AND GRAPHITE FLUORIDE

Watanabe Nobuatsu*

Asaue Teruaki**

ABSTRACT. Research results concerning the anode effect are described. It is concluded that the metal fog connected with the yield depends on the anode effect, but further research is necessary.

1. Introduction

Throughout the entire history of aluminum manufacture and research, the /123*** anode effect has constantly been discussed, and increased importance has gradually come to be attributed to it together with the expansion of the aluminum industry. This is the case, because it exerts a great influence on the manufacturing costs with even slight improvements of the electric power or of the aluminum yield. On the other hand, it is also significant with respect to automation. However, the anode effect is not peculiar to aluminum electrolysis alone; it is a phenomenon which occurs also in fluorine electrolysis using carbon anodes and in chloride fused salt electrolysis. It has an immediate relation to graphite fluoride.

2. The Essence of the Anode Effect

As soon as the anode effect occurs, the bath voltage rises abruptly, there is only flow of the arc current, and it becomes difficult to continue

---

*Faculty of Engineering, Kyoto University (Kyoto-shi, Sakyo-ku, Yoshida Honcho).

**Toyama Works, Sumitomo Chemical Co., Ltd. (Toyama-ken, Shinminato-shi, Kuguminato).

***Numbers in the margin indicate pagination in the original foreign text.

electrolysis. In the electrolysis of aluminum or fluorine, the fluorine ions at the same time scatter in the form of CF_4, which is difficult to recover, and the fluorides are consumed. The anode reaction in a cryolite-alumina system is a competitive reaction between the oxygen ions and the anode surface, and when the fluorine ions are discharged, graphite fluoride is formed and grows on the anode surface [1-3]. Since the discharge of fluorine ions on the carbon anode surface is connected with the anode effect, there is a pronounced similarity [29, 30] between the anode effect phenomenon in aluminum electrolysis [4-21] and the anode effect phenomenon in fluorine electrolysis [22-28]. That is, a carbon-fluorine compound is formed on the anode surface and grows, passing through a number of structures. Finally, a CF compound with an extremely low surface energy spreads all over the entire anode, until it becomes impossible for wetting to occur between the anode surface and the bath. At a high voltage, the only flow which occurs is that of the arc current. However, Holliday et al. [6, 7] think that in normal electrolysis of a cryolite-alumina system, although CF_4 is not produced, when there is a local elevation of the current density, an excess voltage density will occur, and CF_4 will be formed. Once this has been formed, the current distribution will become more and more uneven, and the CF_4 gas film will spread throughout the bath at an accelerated speed. Consequently, they believe that the formation of CF_4 is the cause of the anode effect. On the other hand, Mashovets [31] thinks that anions containing oxygen are discharged on the anode surface and are coupled with the carbon. They are decomposed, passing through intermediate compounds such as C_nO, and become CO_2 or CO. The excess voltage on the anode increases on account of delays in the decomposition of these intermediate products, or on account of adsorption of the gases produced. At a definite current density, an electric potential sufficient for discharge of the ions including fluorine is reached. At this point, the fluorine reacts with the carbon, forming intermediate compounds such as C_nF or C-O-F, and the anode effect occurs. According to him, the formation of CF_4 is not the cause of inactivity of the anode; rather, it is caused by the dismutation reaction of the C_nF. According to Snow et al. [32], the deposition or removal of gaseous products on (or from)

the anode surface is the factor determining the rate, and differences in the carbon structure exert the most important influence on the electric potential causing the anode effect. Furthermore, the speed of deposition or removal of CF_4 varies depending on CO_2. Consequently, they regard the anode effect as occurring due to a slow process of deposition and removal of CF_4, which produces a resistance layer, and they held that the high anode potential occurred as a result of this. In any case, there is agreement in admitting that the fluorine-carbon compounds play a role in the anode effect. On the basis of their research in the electrode reactions of fluorine, the present writers believed that the excess voltages in this reaction include both abrupt excess voltages and slow excess voltages. The latter, they hold, are caused by wetting with the bath resulting from the formation and growth of solid graphite fluoride produced by the reaction between fluorine and carbon. The occurrence of the anode effect was considered to be caused by the formation of graphite fluoride on the anode surface in special cases when this slow overvoltage became extremely great [25]. Graphite fluoride has great electric insulation properties and water- and oil-producing properties. It is a compound which is highly stable with respect to chemicals such as acids and oxidizing agents, and its lubricating properties are highly superior [33]. (Table 1).

The reaction accompanying the discharge of fluorine on the anode surface consists of the following processes.

(1) Movement of fluorine ions from the liquid onto the anode surface.
(2) Discharge reaction of the fluorine ions $F^- \rightarrow F + e$.
(3) Reaction between fluorine and the anode carbon $F + C \rightarrow CF$.
(4) Growth of CF crystals $(CF)_n - I \rightarrow (CF)_n - II$.
(5) Dismutation reaction of CF $4\ CF \rightarrow 3C^* + CF_4 (C_2F_6$ etc.)
(6) Reaction between CF and dissolved aluminum $3CF + Al$ (dissolved) /124
$\rightarrow AlF_3 + C$.
(7) Deposition and removal of CF_4 which has been formed.

TABLE 1. PROPERTY OF GRAPHITE FLUORIDE [33]

	Property of carbon before fluorination				Property of graphite fluoride			
	X ray diffraction half value width	X ray diffraction latice constant (Å)	Specific gravity	Surface area (m^2/g)	Mole ratio (C : F)	Specific gravity	Surface area (m^2/g)	Decomposition temperature (°C)
Natural graphite	1	6.71	2.26	--	1 : 0.97	2.68	193	420
Graphite fiber	48	6.88	1.67	1.5	1 : 0.96	2.52	340	395
Petoroleum coke	17	6.88	20.8	3.8	1 : 0.98	2.50	290	380
Charcoal	—	--	1.68	225	1 : 0.91	2.35	176	333
Binder carbon	740	7.09	1.64	72	1 : 0.92	2.34	180	320
Carbon black	225	6.85	1.88	36	1 : 0.97	2.52	297	390

The quantity of CF formed by the reaction (3) depends on the carbon material, the partial pressure of the fluorine, and the temperature. At higher temperatures, the reaction occurs more briskly, and at the same time the dismutation reaction (5) is also accelerated. The carbon (C*) formed at this time, unlike the original carbon, becomes amorphous [1]. Since the incidence of large quantities of CF_4 is observed when the anode is produced in aluminum electrolysis [8], the reaction proceeds on the anode according to the above-mentioned process: (1) → (2) → (3) → (4) $\nearrow^{(5)}_{\searrow(6)}$, and this eventually leads to the occurrence of the anode effect. The formation of $(CF)_n$ - I is susceptible to the influence of water, but there is no influence of water on $(CF)_n$ - II, which is directly related to the anode effect [34]. Mergault [35, 36] and colleagues state that the anode effect is based on an insulation layer which is strongly adsorbed to the anode graphite. They support the ideas of the present writers.

Two processes must be considered in the formation of the graphite fluoride film on the anode. They are: the formation of anode products, and the simultaneous process of decomposition. The formation reaction depends on the current density and is a function of the electric potential. On the other hand, the decomposition reaction, being a chemical reaction, therefore depends on the temperature, the covering rate, the alumina concentration, and the

dissolved aluminum. But the crystal growth of the graphite fluoride has contents which are connected with both. Let us use the following equation to express the velocity of formation of CF compounds on the anode surface [37-39].

$$d\theta/dt = K_1(1-\theta)f(E) - K_2\theta$$

θ is the ratio of covering with the CF compound. The first term $K_1(1 - \theta)f(E)$ represents the velocity of formation of the CF compound which is formed at $(1 - \theta)$. The second term $K_2\theta$ represents the velocity with which the CF compound formed on the anode surface decomposes according to the dismutation reaction. CF compounds are not produced during normal electrolysis of aluminum, and the only products on the anode may be considered to be carbon oxides. However, when concentration polarization occurs locally, the fluorine ions are discharged there, and CF compounds are produced; next, the dismutation reaction occurs, and CF_4 gas is produced. Holliday et al. [6] measured the CF_4 in the anode gas before occurrence of the anode effect (Table 2). They recognize that the CF_4 concentration increases as the anode effect approaches. Numerous researchers have analyzed the chemical composition of the anode gas at the occurrence of the anode effect; all of them have recognized the occurrence of CF_4 [6-9, 31, 32, 40-45]. In the laboratory electrolysis conducted by the writers, we also confirmed by means of IR spectra the presence of CF_4 in the anode gas [5]. According to Mashovets et al. [8], the quantity of CF_4 amounts to as much as 20% in the anode gas, as may be seen in Table 3; they report that the amount of CO gas produced also increases simultaneously at that time. Holliday [6] also measured the alumina concentration in the bath, the amount of CF_4 produced, and the furnace voltage upon the occurrence of the anode effect in an industrial electrolytic furnace. He gives the results in Table 4. These facts also no doubt prove that the formation of graphite /125
fluoride is the immediate cause of the anode effect.

3. Influence of the Bath Components on the Anode Effect

Baths of the fused salt system have a surface tension greater than those of the aqueous solution system, and the electrodes have a poor wettability

TABLE 2. CARBON TETRAFLUORIDE FORMATION [6].

Time before anode effect (min)	CF_4 content (%)	Current (Amp)
35	0.003	10400
24	0.003	10400
17	0.009	9900
9	0.016	9900

TABLE 3. ANODE GAS COMPOSITION AT ANODE EFFECT [8].

Anode gas composition (%)			
CO_2	CO	CF_4	C_2F_4
21.7	50.6	22.2	2.5
39.7	40.8	17.8	1.7
25.7	52.5	18.3	1.2

TABLE 4. FLUOROCARBON CONTENT OF ANODE GAS INCREASES WITH POTENTIAL AT ANODE EFFECT [6].

Cell current (Amp)	Cell potential (V)	CF_4 content	Cryolite ratio NaF/AlF_3	Al_2O_3 concentration (%)
500	8.7	1.48	1.46	0.63
1000	8.3	1.80	1.57	0.28
1000	8.8	1.85	1.14	0.85
1000	8.0	2.00	1.50	1.00
500	6.2	2.00	1.35	1.00
1000	8.0	2.30	1.50	1.00
500	8.6	2.56	1.46	0.63
1200	10.0	8.00	1.50	1.00
1200	12.0	9.86	1.50	1.00
62000[a]	25.0	12.53	1.48	2.00[b]
53000[a]	27.0	14.70	1.51	2.34

a) Commercial prebake cell

b) Estimated

c) Commercial Söderberg cell.

in the bath. The degree of wettability of the bath on the electrodes is connected with the surface properties of the electrodes and with the properties of the bath. In electrolytic baths of aluminum, the surface tension of the bath varies with changes in the bath components [46]. Consequently, the anode effect is also related to the bath components. As for the condition of bubbles on the carbon electrode in fluorine electrolysis, the contact angle increases together with electrolysis, reaching a highly accelerated rate of increase immediately before the occurrence of the anode effect. Finally, the angle becomes 180°, causing the anode effect [24]. Vajna [9] states that discharge of fluorine ions in aluminum electrolysis brings about an abrupt decline in the wettability of the anode. Gas containing CF_4 spreads over the anode surface, reducing the wettability of the anode surface in the bath. Antipin [10] measured the contact angle on the graphite electrode and found that the wettability of the anode improves together with the increase

in alumina. This supports the finding that the anode effect occurs less readily, the higher is the alumina concentration. As for the relationship between bubble size and the contact angle, other researchers have also conducted similar considerations [24, 48, 49]. Belyaev [46] sought the relationship between the critical current density, the contact angle, and the surface tension in an NaF-AlF_3 system and found that with the increase in the AlF_3 components there was an increase of the contact angle and a decrease of the /126
critical current density, as is shown in Figure 4. As for the wettability during polarization, in a cryolite-alumina system, a drop was put on a graphite plate as shown in Figure 5 and polarized in an argon atmosphere. It was observed that pronounced differences in the shape of the drops existed between the anode (A) and the cathode (B) [50]. In (A), the contact angle between the graphite plate and the drop is extremely great, and there is poor wettability between the liquid and the anode. In (B), there is a small contact angle between the graphite plate and the drop, and this proves that there is very good wettability. Figures 6 - 8 indicate the relationship between the AlF_3 concentration and the contact angle, the Al_2O_3 concentration and the contact angle, the time and the potential.

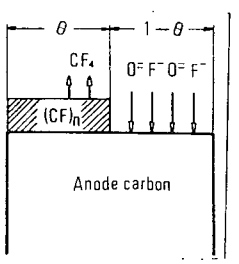

Figure 1. Model of wettability on anode.

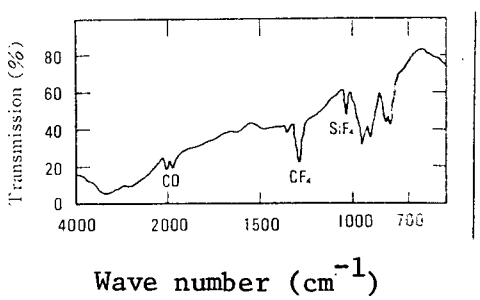

Figure 2. IR spectra of anode gas.

In fused salt electrolysis using carbon anodes, the anode effect occurs at a relatively low current density, especially in systems where fluorides are present. However, in other haloid salts the critical current density assumes

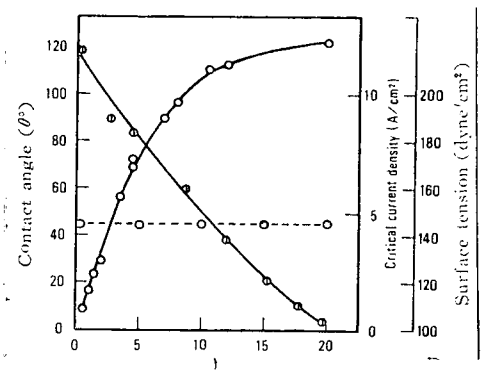

Alumina concentration (wt%)

O: Critical current density
●: Contact angle
●: Surface tension

Figure 3. Relation between alumina concentration (wt%) and contact angle (θ^0), critical current density (A/cm^2), surface tension (dyne/cm) in Na_3AlF_6 - Al_2O_3 system.

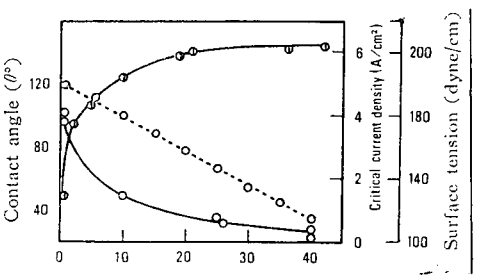

AlF_3 (mol %)

O: Critical current density
●: Contact angle
●: Surface tension

Figure 4. Relation between AlF_3 (mol%) and contact angle (θ^0), critical current density (A/cm^2), surface tension (dyne/cm) in NaF - AlF_3 system.

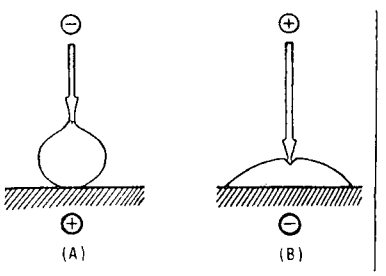

(A) Anodic polarization

(B) Cathodic polarization

Current: I = 0.01 Amp

Cryolite drop: 2.5 NaF·AlF_3

Figure 5. Shape of fused dryolite drop.

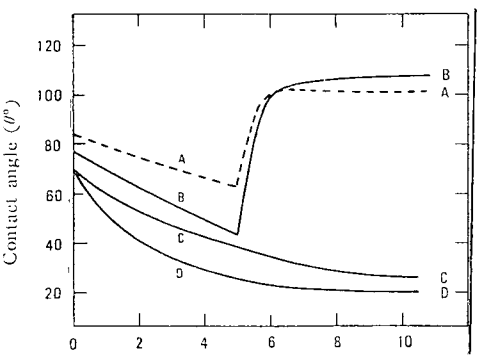

Time (min)

A: Pure cryolite B: 2wt% Al_2O_3

C: 6wt% Al_2O_3 D: 10wt% Al_2O_3

Figure 6. Relation between contact angle (θ^0) and time (min) on graphite anode in Na_3AlF_6 - Al_2O_3 system when anode is polarized for different alumina concentration.

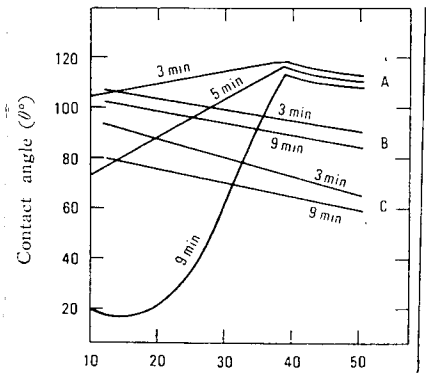

AlF_3 (wt%)

A: I = 0

B: I = 0.0225 amp anodic polarization

C: I = 0.0225 amp cathodic polarization

Figure 7. Relation between contact angle (θ^0) and AlF_3 (wt%) in $NaF - AlF_3$ system when current I = 0, and I = 0.0225 amp.

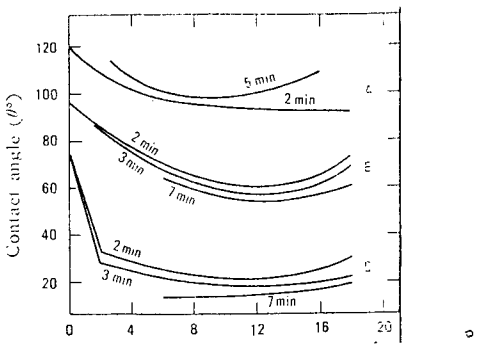

Alumina concentration (wt%)

A: I = 0

B: I = 0.3 amp anodic polarization

C: I = 0.3 amp cathodic polarization

Figure 8. Relation between contact angle (θ^0) and alumina concentration (wt%) in $Na_3AlF_6 - Al_2O_3$ system when current I = 0 and I = 0.3 amp.

a higher value. It has also been reported by many researchers [4, 5, 9, 11-13, 32, 46, 52-62] that there is an increase in the critical current density when the alumina concentration in the electrolytic bath increases. It is explained that the anode effect will not occur when there is discharging of the oxygen ions only, as long as discharging of the fluorine ions does not take place. In other systems as well, the presence of oxides exerts a great influence on the critical current density. Concerning cryolite-alumina systems, numerous equations have been proposed for the relationship applying between the critical current density and the oxide contents in the bath. Vajna [9] and Thonstad [57] hold that there is a linear relation between the critical current density /127 and the alumina concentration. Piontelli [56] and Belayev [11, 47, 58] hold that the critical current density is in direct proportion to the square root of the alumina concentration, and Schischkin [12] concluded that it is in direct proportion to the cubic root.

4. Cell Voltage

When the temporal changes of the cell voltage in a cryolite-alumina system are observed, one obtains a voltage fluctuation diagram with a regular saw-tooth pattern such as that shown in Figure 10. When the alumina at this time is added in the vicinity of the anode, the voltage amplitude abruptly decreases, and the voltage becomes stabilized. When this fact is considered from the standpoint of the effect of addition of LiF in fluorine electrolysis [27], the alumina colloid which is positively charged in the bath is adsorbed to the negatively charged gas bubbles on the anode surface, and this decreases the interfacial energy. That is, the gas bubbles are neutralized by the colloid, the electrostatic attraction with the anode surface becomes smaller, and it becomes easier for the bubbles to leave the anode surface. The voltage thus becomes stabilized. When they are completely dissolved, the original saw-tooth wave form is resumed. The addition of alumina has a more pronounced effect in reducing the cell voltage the higher is the current density (Figure 11). Decreases of the cell voltage are observed even when oxides other than alumina (Zr_2O_3, CeO_2, SiO_2) are added to the cryolite bath [5] (Table 7). In addition, colloid product or additive salts have the effect of increasing the critical current density also in the electrolysis of fused table salt. In view of this point, doubts remain about whether the voltage decrease can be explained in terms of the supply of oxygen ions alone. This is because it is clear from Figure 12 and Figure 13 that the critical current density becomes smaller when the fluorine ion concentration increases [46, 55, 63, 64].

The cell voltage in aluminum electrolysis is represented by the following formula

$$E = E_0 + \eta + eD\gamma + IR_1 + IR_2 + E_{AE}$$

Here E_0 is the theoretical cell voltage, η the excess voltage, e the distance between poles, D the current density, γ the resistibility, R_1 the cell resistance, R_2 the external circuit resistance, I the current, and E_{AE} /129

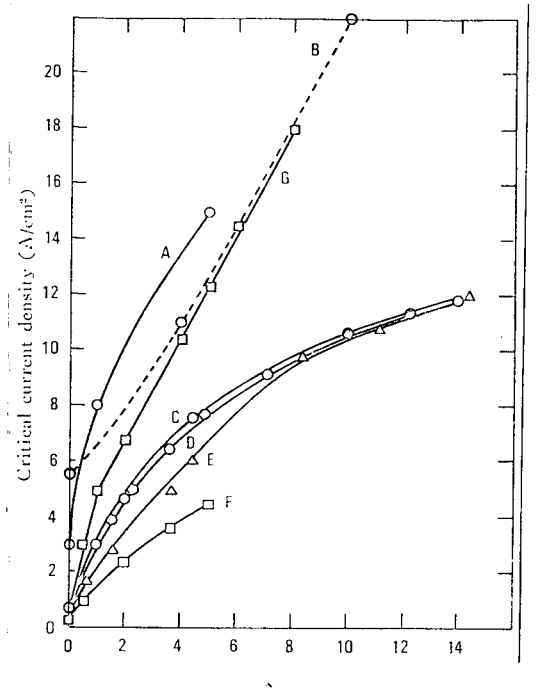

Alumina concentration (wt%)

A: Arndt and Probst, B: Tverdovskii and Zhivov, C: Abramov and Kalyzhiskii, D: Belayev and Kyzhimin, E: Karpachev, Dologov and Kanchinskii, F: Schischkim, G: Thonstad

Figure 9. Relation between alumina concentration (wt%) and critical current density (A/cm2) in Na_3AlF_6 - Al_2O_3 system.

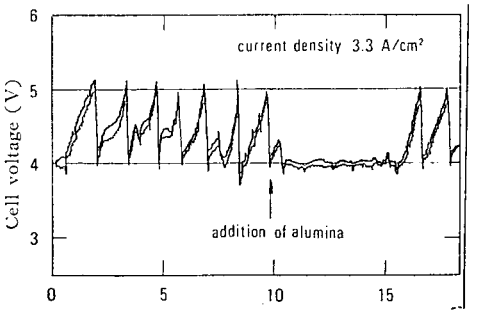

Time (sec)

Figure 10. Change of cell voltage.

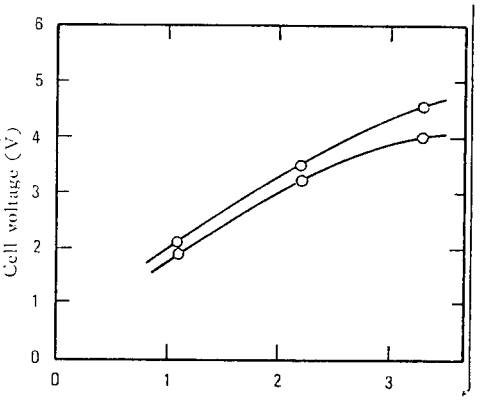

Anode current density (A/cm^2)

O: Without addition of alumina
O: With addition of alumina

Figure 11. Effect of addition of alumina on cell voltage.

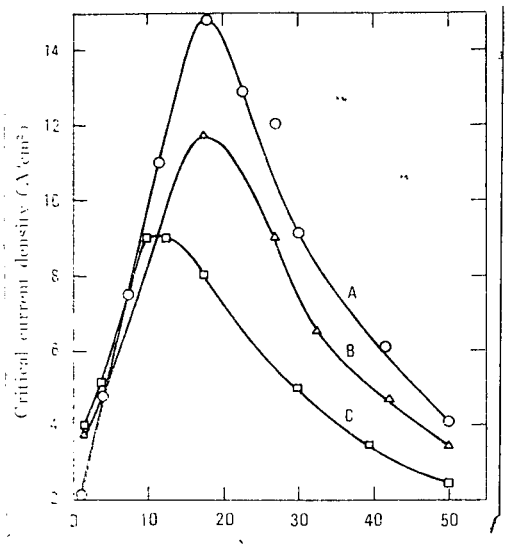

Alumina concentration (wt%)

A: $3NaF \cdot AlF_3$, B: $2.7NaF \cdot AlF_3$,

C: $2.2NaF \cdot AlF_3$.

Figure 12. Effect of alumina concentration (wt%) on critical current density (A/cm^2) for different cryolite ratio.

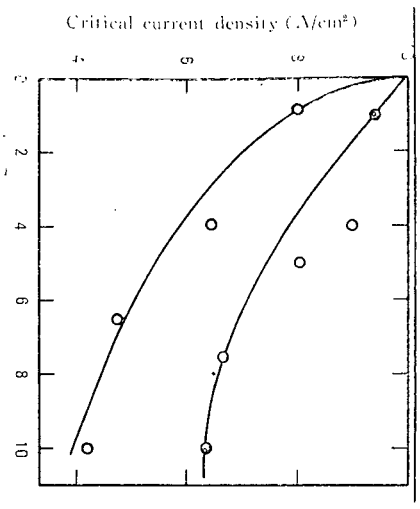

Concentration (wt%)

O: CaF_2, : MgF_2

Figure 13. Relation between critical current density and fluoride concentration in 2.5 $NaF \cdot AlF_3$ + 5%Al_2O_3 system at 1000° C.

TABLE 5. WETTABILITY AND CRITICAL CURRENT DENSITY IN CRYOLITE ALUMINA SYSTEM [46]

Electrolyte	Temperature (℃)	Anode material	Critical current density (A/cm^2)	Surface tension γ(dyne/cm)	Contact angle θ(degree)	Wettability $W=\gamma(H\cos\theta)$
Na_3AlF_6	1000	Carbon	0.45	145	138	45
Na_3AlF_6	1000	Graphite	0.31	145	144	25
Na_3AlF_6+5% Al_2O_3	1000	Carbon	8.65	145	80	170

TABLE 6. CRITICAL CURRENT DENSITY FOR DIFFERENT ELECTROLYTES [26]

Electrolyte	Temperature (℃)	Critical current density (A/dm^2)
NaF	1000	90
NaCl	810	1030
NaBr	800	>5000
NaI	800	>3000

TABLE 7. EFFECT OF ADDITION OF ADDITIVES ON CELL VOLTAGE

Additives	Cell voltage (V)	Variance of cell voltage (V)	cell voltage (V)	Variance of cell voltage (V)	Difference of cell voltage (V)
Al_2O_3	4.3	1.2	3.8	0.3	0.5
Zr_2O_3	4.5	1.2	4.0	0.3	0.5
CeO_2	4.1	0.9	3.7	0.3	0.4
SiO_2	4.4	1.2	3.9	0.3	0.5

the mean voltage drop due to the anode effect. The factors bringing about increase of the voltage are the increases of eD/γ, IR_1, and IR_2, respectively, due to increases of the current, and increases of the excess voltage η. The increase of the voltage up to the occurrence of the anode effect is brought about chiefly by the increase in the above-mentioned slow excess voltage [25, 64]. In a cryolite-alumina system, from the current-potential curve, the anode effect occurrence potential and the extinction potential assume more or less identical values, as is shown in Figure 14 [5]. This means that there is a definite potential which is the boundary value beyond which graphite fluoride occurs, grows, and disappears on the anode surface. When the temperature is raised, generally the diffusion, electric conductivity, and solubility of ions increase, while on the contrary, the viscosity and surface tension become lower. If the reaction preceding the anode effect governs the diffusion, the diffusion is accelerated as the bath temperature rises. The replenishment of the oxygen ions is accelerated together with the increase of the solubility of alumina, while the critical current density at which the anode effect occurs becomes higher (Figure 15). The formation of graphite fluoride and the decomposition reaction velocity also increase. The effects of the temperature on the critical voltage are shown in Table 8. Concerning the anode effect in cryolite-alumina systems, Piontelli et al. [55] state that when mechanical vibrations are administered to the anode, the critical current density will rise, and the anode effect will have a great influence on the shape and behavior of the anode. Further, in anodes of a cylindrical or spherical shape, in which gas discharge in the anode is easy, the critical current density at which the anode effect occurs will become greater. They gave the following formula for the relationship between the anode shape and the current density (Ic).

$$I_c = \varphi(a - bT)\cdot A^n\{c+[Al_2O_3]^m\}$$

Here, a, b, c, m, and n are constants. A is the apparent anode area (cm^2). T is the temperature (° C), and $[Al_2O_3]$ is the alumina concentration (wt%). ϕ is a coefficient depending on the anode shape; the values are shown

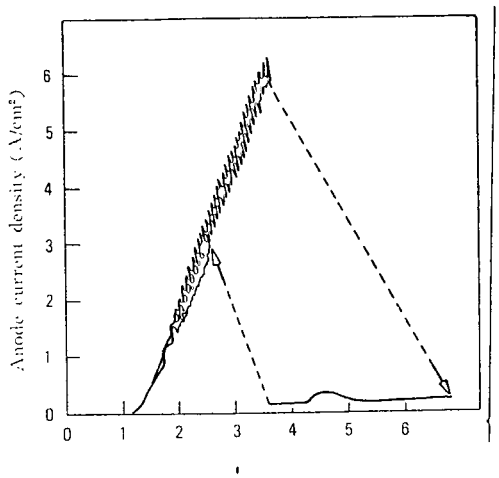

Anode: Graphite

Alumina concentration: 4wt%

Scan rate: 0.1 V/sec

Figure 14. Current potential curve by potential sweep method in Na_3AlF_6 - Al_2O_3 system.

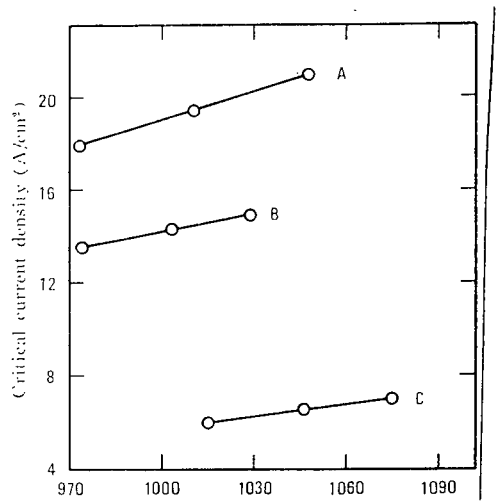

A: 12wt%, B: 8wt%, C: 15wt%

Figure 15. Critical current density as a function of temperature for different alumina concentration.

TABLE 8. RELATION BETWEEN TEMPERATURE AND CRITICAL VOLTAGE FOR VARIOUS ALUMINA CONCENTRATION [32]

Al_2O_3 concentration (wt%)	Temperature (℃)	Critical voltage (V)
1.9	1014	5.16±0.04
2.0	1027	5.06±0.07
5.0	1034	8.01±0.13
5.0	1057	8.57±0.14
6.0	1051	9.15±0.06

TABLE 9. VALUES OF ϕ FOR VARIOUS ANODE SHAPES [54]

Anode shape	φ
Horizontal (downwards)	1
Hemispherical	1.4
Cylindrical	1.3
Concave	0.5~0.55

in Table 9. As shown in Table 10, the critical potential and the critical current density at which the anode effect occurs differ depending upon the anode material (Figure 16). In fluorine electrolysis as well, when the degree of graphitization surpasses 50%, the anode effect occurs more readily; it

TABLE 10. EFFECT OF ELECTRODE CARBON ON CRITICAL CURRENT DENSITY [32]

Alumina concentration (wt%)	Morganite graphite (A/cm^2)	Union carbide graphite (A/cm^2)
4.00	7.00	10.50
7.00	11.40	14.50
8.00	11.80	13.20
10.00	16.30	—

TABLE 11. CRITICAL CURRENT DENSITY FOR DIFFERENT DEGREE OF GRAPHITIZATION [29]

Degree of graphitization (%)	Critical current density(A/cm^2)	
	KF·2 HF	KF·2 HF+3 wt% Al_2O_3
0~10	5~10	18~22
10~30	5~8	18~22
30~50	4~8	18~22
50~70	2~4	4~5
70 up	1~2	1~2

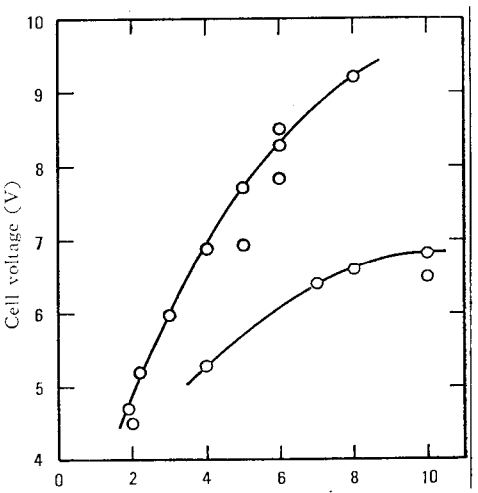

Alumina concentration (wt%)

○: Union Carbide, AVC graphite

●: Morganite, EY9 graphite

Figure 16. Cell voltage alumina concentration curve for different electrode chains.

occurs less readily, the more carbonaceous is the material [29]. This is because the reactions for formation and decomposition of graphite fluoride occurring on the anode surface differ depending on the divergences in the crystallinity of the carbon [6]. This explanation fits the facts well.

5. Conclusion

We have introduced a few of the many research results concerning the anode effect and explained our own personal opinions in connection with graphite fluoride. However, this does not mean that the essence of the anode effect has been elucidated. The writers also believe that the metal fog which is connected with the yield is not independent of the anode effect. For the sake of further improvements and development of the aluminum industry, further research and information will be necessary concerning the anode effect phenomenon as well as the electrode reaction mechanism in the anode and cathode.

REFERENCES

1. Nobuatsu, Watanabe, Koyama Yoshiyuki and Yoshizawa Shiro. This Journal Vol. 31, 1963, p. 756.

2. Nobuatsu, Watanabe and Kobun Kiyoshi, ibid. Vol. 35, 1967, p. 19.

3. Nobuatsu, Watanabe and Shibuya Atsuyoshi. Koka [abbreviation of Kogyo kagaku (Industrial Chemistry)]. Vol. 77, 1968, p. 963.

4. Nobuatsu, Watanabe and Ohniwa Nobuhiro. This Journal, Vol. 35, 1967, p. 178.

5. Nobuatsu, Watanabe, Kato Fumikazu and Ohmura Keigo, ibid. Vol. 37, 1969, p. 274.

6. Holliday, R.D. and J.L. Henry. Ing. Eng. Chem. Vol. 51, 1959, p. 1289.

7. Holliday, R.D. and J.L. Henry. J. Metals N.| Y., Vol. 9, 1957, p. 1384.

8. Moshovets, V.P. and E.D. Zhaharov. Zhur. Priklad. Khim., Vol. 29, 1956, p. 1512.

9. Vajna, A. Bull. Soc. franc. electriciens, Vol. 2, 1952, p. 85.

10. Antipin, L.N. and S.F. Vazhenin. Zhur. Priklad. Khim., Vol. 31, 1958, p. 1103. /130

11. Belayev|, A.I. Khim. Referate. Zhur., Vol. 4, No. 5, 1941, p. 83.

12. Schischkin, V. Z. Elektrochem., Vol. 33, 1927, p. 83.

13. Drossbach, P. and P. Krahl. Zur. Kenntnisdes. Anodeneffeckts (Knowledge of the Anode Effect). Diss Technische Hochschule Munchen, 1959.

14. Drossbach, P. and P. Krahl. Z. Elektrochem., Vol. 62, 1958, p. 178.

15. Drossbach, P. Z. Elektrochem., Vol. 60, 1956, p. 387.

16. Antipin, L.N. and N.G. Turpin. Zhur. Fiz. Khim., Vol. 31, 1957, p. 1130.

17. Ginsberg, H. and A. Böhm. Z. Elektrochem., Vol. 61, 1957, p. 315.

18. Rempel, S.I. and L.P. Khodak. Doklad. Akad. Nauk SSSR, Vol. 75, 1950, p. 833.

19. Rempel, S.I. Doklad. Akad. Nauk SSSR, Vol. 76, 1951, p. 411.

20. Antipin, L.N. and A.N. Khudyakov. Zhur. Priklad. Khim., Vol. 29, 1956, p. 908.

21. Belyaev, A.I. and L.A. Firsanova. Zhur. Priklad. Khim., Vol. 31, 1958, p. 1361.

22. Nobuatsu, Watanabe, Otto Taibun and Yoshizawa Shiro. This Journal, Vol. 29, 1961, p. 245.

23. Nobuatsu, Watanabe, Ishii Masato and Yoshizawa Shiro. Ibid., Vol. 29. 1961, p. 492.

24. Nobuatsu, Watanabe, Ishii Masato and Yoshizawa Shiro. Ibid., Vol. 29, 1961, p. 497.

25. Nobuatsu, Watanabe, Ishii Masato and Yoshizawa Shiro. Ibid., Vol. 30, 1962, p. 171.

26. Nobuatsu, Watanabe, Fujii Yoshihiko and Yoshizawa Shiro. Ibid., Vol. 31, 1963, p. 611.

27. Nobuatsu, Watanabe, Inoue Mamoru and Yoshizawa Shiro. Ibid., Vol. 31, 1963, p. 762.

28. Nobuatsu, Watanabe and Nishimura Masakatsu. Yoyuen (Fused Salts), Vol. 11, No. 2, 1968, reprint.

29. Nobuatsu, Watanabe and Ishii Masato. This Journal, Vol. 29, 1961, p. 364.

30. Nobuatsu, Watanabe and Yoshizawa Shiro. Ibid., Vol. 32, 1964, p. 90.

31. Mashovets, V.P. Zhur. Priklad. Khim., Vol. 31, 1958, p. 571.

32. Snow, R.J. and B.J. Welch. Proc. Aust. Inst. Min. Met., No. 221, 1967, p. 43.

33. Nobuatsu, Watanabe. Seramikkusu (Ceramics), Vol. 4, 1969, p. 301.

34. Nobuatsu, Watanabe, Tasaka Akimasa and Nakayama Hidetoshi. Denki Kagaku Kyokai Dai-37-kai Taikai Koen Yoshi (Abstracts of Lectures at the 37th Congress of the Electrochemistry Association), Vol. 5 B, 1970, p. 312.

35. Mergault, P. Comp. rend., Vol. 240, 1955, p. 756.

36. Mergault, P. Comp. rend., Vol. 250, 1960, p. 849.

37. Srinivasan, S. and E. Gileadi. Electrochimica Acta, Vol. 11, 1966, p. 321.

38. Thonstad, J. Electrochimica Acta, Vol. 13, 1968, p. 449.

39. Lovrecek, B. and K. Moslavac. Electrochimica Acta, Vol. 13, 1968, p. 174.

40. Pearson, T.G. and J. Waddington. Discuss. Faraday Soc., Vol. 1, 1947, p. 307.

41. Thonstad, J. Electrochimica Acta, Vol. 14, 1969, p. 127.

42. Treadwell, W.D. and A. Kohl. Helv. Chim. Acta, Vol. 9, 1926, p. 681.

43. Rempel, S.I. Doklad. Akad. Nauk SSSR, Vol. 117, 1957, p. 648.

44. Antipin, L.N. and V.K. Dudyrev. Zhur. Fiz. Khim., Vol. 31, 1957, p. 2032.

45. Antipin, L.N., S.F. Vazhenin and A.A. Sinyagov. Izvest. Vysshikh. Ucheb. Zavedenii Tssvetnaya Met., No. 5, 1958, p. 62.

46. Belyaev, A.I., E.A. Zhemchuzhina and L.A. Firsanova. Yoyuen no butsuri kagaku (Physico-Chemistry of Fused Salts), Moscow, 1957.

47. Bloom, H. and B.W. Burrous. Electrochemistry Proc. Inst. Aust. Conf., Pergamon Press, London, 1964, pp. 901-922.

48. Kabanov, B. and A. Frumkin. Z. Physik. Chem., Vol. A165, 1933, p. 433.

49. Kabanov, B. and A. Frumkin. Z. Physik. Chem., Vol. A166, 1933, p. 316.

50. Belyaev, A.I. and E.A. Zhemchuzhina. Izv. Vuzov. Tsvet. Metallurg., Vol. 4, No. 5, 1961, p. 123.

51. Belyaev, A.I. and E.A. Zhemchuzhina. Izv. Vuzov. Tsvet. Metallurg., Vol. 5, No. 1, 1962, p. 82.

52. Schmitt, H. Extractive Metallurgy of Aluminum, Vol. 2, Aluminum G. Gerala Edition, Interscience Publisher, New York, 1963, p. 169.

53. Piontelli, R. Proceeding of the First Australian Conference on Electrochemistry, Gutman and Friend, Editors, Pergamon Press, London, 1964, p. 932.

54. Welch, B.J. and R.J. Snow. J. Electrochemical Soc., Vol. 113, 1966, p. 1338.

55. Piontelli, R., B. Mazza and P. Pedeferri. Electrochimica Acta, Vol. 10, 1965, p. 1117.

56. Thonstad, J. Electrochimica Acta, Vol. 12, 1967, p. 1219.

57. Belyaev, A.I., E.A. Zhemchuzhina and A.P. Gersimov. Zhur. Priklad. Khim., Vol. 29, 1956, p. 1843.

58. Abramov, G.A., M.M. Vetyukov, I.P. Gupalo, A.A. Kostykov and L.N. Loshkin. Teoretceskiye osnovy electrometallurgii alumina (Theoretical Bases of Alumina Electrometallurgy). Metallurgizdat, Moscow, 1953, p. 350.

59. Belyaev, A.I., M.B. Rapoport and L.A. Firsanova. Metallurgie des Aluminums (Aluminum Metallurgy). Technik Berlin, 1956, p. 122.

60. Matiasovsky, K., V. Damek and M. Malinovski. Chemicke Zvesti, Vol. 17, 1963, p. 211.

61. Krohn, C.H. Tidsski Kjem Bergr Metall., Vol. 21, 1961, p. 62-

62. Drossbach, P., T. Hashino, P. Krahl and W. Pfeiffer. Chemie. Ing. Techn., Vol. 33, 1961, p. 84.

63. Belyaev, A.I., E.A. Zhemchuzhina and L.A. Firsanova. Physikalische chemie geschmolzemer salze (Physical Chemistry of Molten Salts). Grundstoffindustrie Leipzig, 1964, p. 322.

64. Wasilewski, L. and L. Piszczek. Chem. Stosowana, Ser. A 8, No. 2, 1964, p. 223.

65. Haupin, W.E. J. Electrochemical Soc., Vol. 103, 1956, p. 174.

Translated for National Aeronautics and Space Administration under Contract No. NASw 2035, by SCITRAN, P.O. Box 5456, Santa Barbara, California, 93108.